Supplemental Material

Microfluidic-based ^{18}F-labeling of Biomolecules for ImmunoPET

Kan Liu[1-4,7], Eric J. Lepin[2-4,7], Ming-Wei Wang[2-5], Feng Guo[2-4,6], Wei-Yu Lin[2-4], Yi-Chun Chen[2-4], Shannon J. Sirk[2-4] , Sebastian Olma[2-3], Michael E. Phelps[2-4], Xing-Zhong Zhao[6], Hsian-Rong Tseng[2-4], R. Michael van Dam[2-4,8], Anna M. Wu[2-4,8] and Clifton K.-F. Shen[2-4,8]

[1]College of Electronics and Information Engineering, Wuhan Textile University, Wuhan, 430000, China.

[2]Department of Molecular and Medical Pharmacology, David Geffen School of Medicine at University of California, Los Angeles, 23-120 Center for Health Science, Los Angeles, California 90095, USA.

[3]Crump Institute for Molecular Imaging, 570 Westwood Plaza, Los Angeles, California 90095, USA.

[4]California Nanosystems Institute, 570 Westwood Plaza, Los Angeles, California 90095, USA.

[5]PET Center and Department of Nuclear Medicine, Cancer Hospital, Fudan University, Shanghai, 200032, China.

[6]Department of Physics, School of Physics, and Center of Nanoscience and Nanotechnology, Wuhan University, Wuhan 430072, China.

[7]These authors contributed equally to this work.

[8]Correspondence and reprint requests should be addressed to C.K.-F.S. (kshen@mednet.ucla.edu), A.M.W. (awu@mednet.ucla.edu) and R.M.V. (mvandam@mednet.ucla.edu).

Table of Content

Chip Fabrication and Setup

The microfluidic chips used in this study were implemented as a two-layer polydimethylsiloxane (PDMS) microfluidic chip similar to published procedures, summarized briefly as follows.[1] The channels on the upper layer are flow microchannels used for the reagent inlets, filling chambers, and output of generated droplets, while the channels on the lower layer are control channels that can be pressurized or depressurized to open or close the corresponding microvalve(s). Silicon wafer molds composed of photoresist-patterned microstructures for fabrication of the fluid and control layers were created by standard photolithographic techniques. Both molds were pretreated with trimethylsilyl chloride (TMSCl) vapor for 10 min to facilitate the release of final PDMS replica. Well-mixed PDMS pre-polymer (GE RTV615, total weight: 36g, mixing ratio: A:B = 5:1) was poured onto the fluid layer mold to give a 6mm-thick fluidic layer with approximately 40 μm channel depth. Another portion of PDMS pre-polymer (GE RTV615, total weight: 10g, mixing ratio: A:B = 20:1) was mixed and then spin-coated onto the control layer mold at 1500 RPM for 60 s. The fluidic and control layers were cured at 80°C for 15 min and 18 min, respectively. After baking, the fluidic layer replica was peeled from the mold, aligned onto the control layer, and then the assembly was baked at 80°C for at least 6 h to adhere the layers. The chip was peeled off of the mold when the fluidic and control layers were firmly bonded together. Holes were then punched to form ports connected to the fluidic layer channels for reagent inlets and outlets, and ports connected to the control layer channels for microvalve and pump actuation with hydraulic fluid (water). Adhesion of the chip to a clean glass microscope slide to seal the control channels was achieved by corona discharge treatment. The microfluidic device was baked in an oven at 80°C for 72 h to restore the intrinsic hydrophobicity of PDMS surfaces which is needed to minimize reagent loss and non-specific binding of biomolecules on channel walls when moving aqueous droplets.

Microvalve control lines were filled with water as hydraulic fluid. Microvalves were actuated by pressurizing the corresponding control channels (up to 60 psig) via electronic solenoid valves (Series S070, SMC, Toyko, Japan). All valves were automatically controlled through a data acquisition module (USB-4750, Advantech, USA) driven by a custom software program written in LabView (National Instruments, USA). The microfluidic system includes two microfluidic chips (a distribution chip of pH buffers and a digital microfluidic droplet generation (DMDG) chip connected by tubing). The DMDG chip is composed of three functional parts (**Fig. 1B**): (1) a droplet generation core, where specific quantities of reagents are measured and merged into composition-specific droplets; (2) a peristaltic pump, which produces serial compressed nitrogen pulses that can precisely deliver intact droplets to the desired location and (3) a mixing channel. **Figure S1** shows the external solution distribution chip (**Fig S1a**) and the droplet generation core (**Fig. S1b)**.

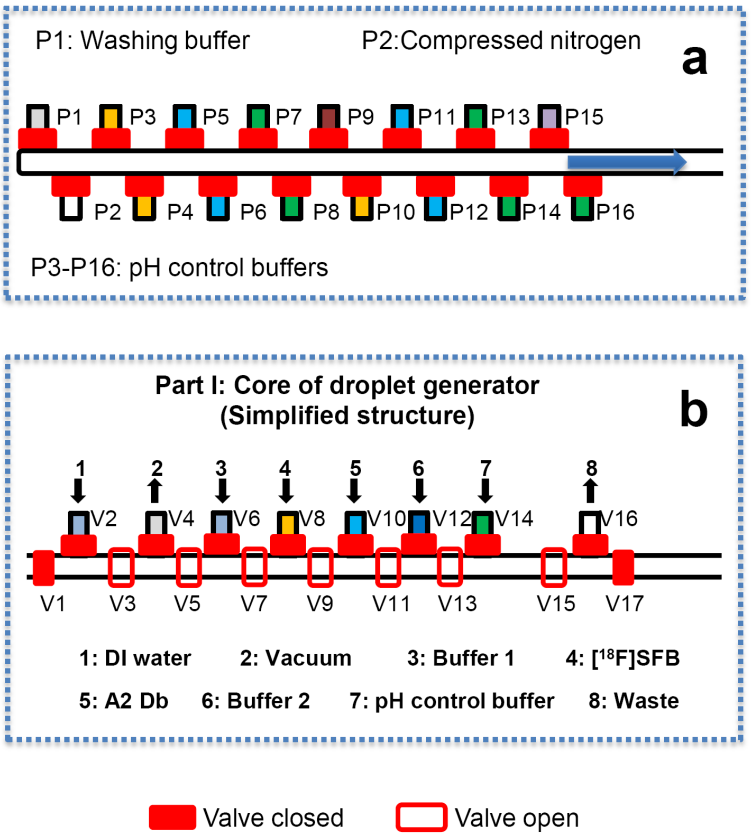

Figure S1. (**a**) The distribution chip includes one washing buffer channel, one compressed nitrogen channel (for pushing out pH buffers) and fourteen different pH buffer inlets that provide pH control buffers. (**b**) The digital microfluidic droplet generator core includes five reagent inlets, one vacuum inlet, one washing inlet, one waste outlet, one compressed nitrogen inlet and one droplet outlet. All the reagents are loaded into the chip by compressed nitrogen.

The unique features of our DMDG chip (**Fig. 1B**) are: (1) independent control of volume and composition for every droplet, enabling screening with minimal reagent consumption; (2) ability to pause, modify, and restart the droplet generation process, e.g. for replacement/change of reagents; and (3) the use of nitrogen gas rather than oil to separate droplets, eliminating the need for oil removal steps afterward. Using the microvalves to isolate each reagent inlet, the incoming

reagents are not in contact with each other until the moment of droplet formation. They will be rapidly mixed and reacted thereafter while moving along the microfluidic channel. This is particularly critical because some radiolabeling tags, such as [^{18}F]SFB, are often unstable and prone to hydrolyze/decompose at higher pH.

Anti-PSCA A2 Diabody

Prostate stem cell antigen (PSCA) is a cell surface glycoprotein over-expressed in prostate cancer. Over 80% of human prostate cancers examined, including local disease and the metastatic bone lesions, express PSCA. We have previously demonstrated that different antibody fragments derived from humanized 2B3 anti-PSCA antibody including minibodies (80 kDa) and diabodies (50 kDa) labeled with I-124 were able to specifically image PSCA-expressing xenografts in mice by microPET. Humanization resulted in a loss of affinity compared to the parental monoclonal antibody, necessitating affinity maturation using molecular evolution by yeast display. 2B3 single chain Fv variants were generated by error-prone PCR and were expressed as a library on the surface of yeast cells. Three yeast clones with improved affinity, A2, A11 and C5, were selected with A2 demonstrating highest affinity. The A2 diabody construct was generated by fusing the V_H and V_L domain with a 5 amino acid linker and a 6 histidine Tag was added to the C-terminus for purification and detection. The protein sequence of A2 diabody is presented below. A2 diabody was purified using Ni-NTA affinity chromatography. To measure the pH stability of A2 diabody, we incubated the protein at different pH values from 7.4 to 9.8 for 30 min. The pH was then neutralized to pH 7.4 using 1M Tris-HCl pH 7.4. Binding to recombinant PSCA protein was measured by ELISA (A2 diabody was detected with an AP conjugated anti-Myc monoclonal antibody (Invitrogen). Results are presented in Figure S2 as a percentage of maximum binding.

The protein sequence:

DIQLTQSPSSLSASVGDRVTITCSASSSVRFIHWYQQKPGKAPKRLIYDTSKLASGVPSRFS
GSGSGTDFTLTISSLQPEDFATYYCQQWGSSPFTFGQGTKVEIKGSTSGGGSEVQLVESGG
GLVQPGGSLRLSCAASGFNIKDYYIHWVRQAPGKGLEWVAWIDPEYGDSEFVPKFQGR
ATMSADTSKNTAYLQMNSLRAEDTAVYYCKTGGFWGRGTLVTVSSAAAEQKLISEEDL
NGAAHHHHHH

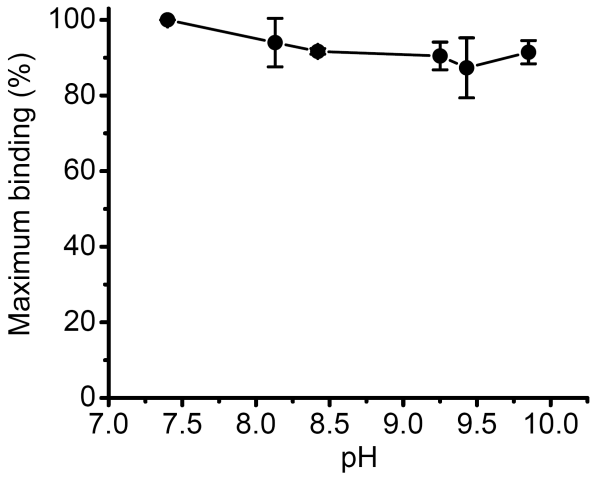

Figure S2. The stability of A2 diabody (as measured by PSCA binding) in different pH buffers for 30 min (n=3).

Radiosynthesis of [^{18}F]SFB

[^{18}F]SFB has been synthesized and produced routinely by a one-pot, microwave-assisted procedure. Briefly, modified from the published procedures, we have developed a simplified radiosynthesis using an anhydrous deprotection strategy and microwave heating.[2] This three-step process can be performed in a one-pot matter thus shortens the reaction time (< 60 minutes). The final radiochemical yield (RCY) of [^{18}F]SFB is about 30-40% (n>30) with a radiochemical purity >98% after radio-HPLC purification. The [^{18}F]SFB is concentrated on a polystyrene cartridge and eluted with diethyl ether. After solvent removal, [^{18}F]SFB is reconstituted in PBS buffer (pH 7.4) before loading onto microfluidic chips for optimizing labeling reaction parameters (**Fig. 1C**).

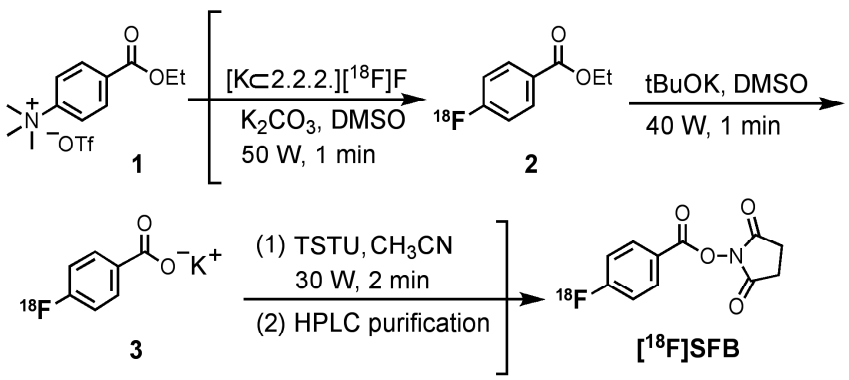

Figure S3. The one-pot microwave-assisted [^{18}F]SFB synthesis.

pH Stability Test of [^{18}F]SFB

The stability of [^{18}F]SFB in different pH buffer was measured (**Fig. S4**). 10 different pH buffer solutions (50 μL) were loaded into 10 individual V-vials. [^{18}F]SFB (5 μL) was immediately added into each vial. Sequentially, the samples were injected into HPLC for analysis after 10 min. In the case of stability test in pH 7.4 buffer, the samples were analyzed at various of time points (10, 20, 30, 60 and 120 min). The percent decomposed [^{18}F]SFB vs intact [^{18}F]SFB at different time points were plotted. [^{18}F]SFB remained stable (>90%) in pH 7.4 buffer after 2 h.

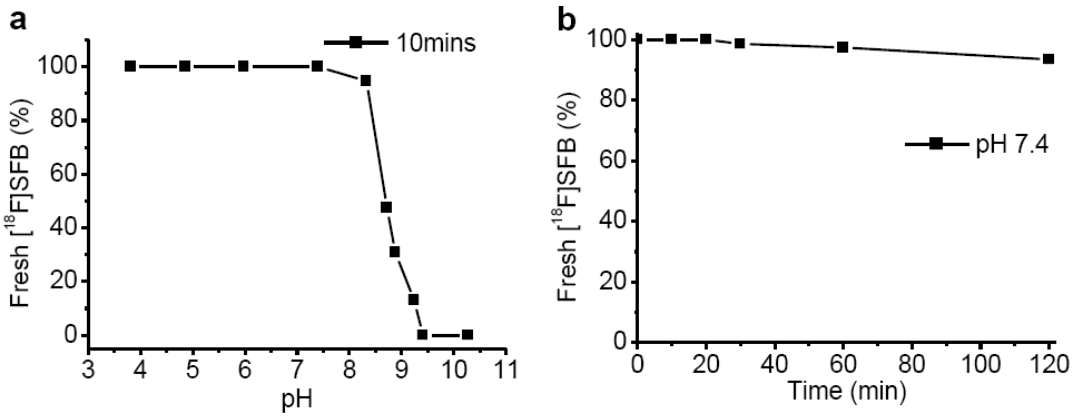

Figure S4. (**a**) [^{18}F]SFB stability in different pH buffers for 10 min is shown. (**b**) The stability of [^{18}F]SFB in pH 7.4 buffer over 2-hour time period.

Droplet Generation and Washing Process

Figure S5 describes the main features and step-by-step operation of droplet generation. A droplet composed of several reagents in well-defined volume ratios can be generated in each cycle by running the steps of **Table S1**. In **Figure 1D**, section I is used for [^{18}F]SFB, section II for A2 Db and buffer 2, section III for pH control buffer, respectively. The detailed operation sequence showing valve states for droplet generation: (i) the filling chambers are evacuated (*ca.*-75 kPa) to remove air and thereby accelerate filling (*ca* 100 ms); (ii) the reagents are driven into these chambers by positive pressure (*ca.* 172 kPa; 100 ms-60 s); (iii) the reagents are merged into a single end-to-end multi-component droplet (*ca* 100 ms) and (iv) pushed out of the reagent filling chambers via a series nitrogen gas pulses (*ca.* 35-172 kPa) from an on-chip peristaltic pump (*ca* 100 ms-10 s). A sealing step (50 ms) is inserted after each step to compensate for any slight variations in valve response times and ensure no cross-contamination of reagents. Because reagents are filled into isolated chambers with well-defined conditions, droplet formation is therefore not affected by long-range hydrodynamic interactions or the "history" of previously generated droplet (as is the case in continuous flow devices), enabling every single droplet to be precisely and independently controlled.

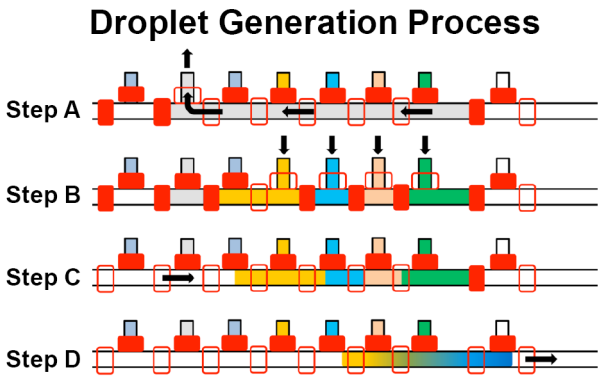

Figure S5. Droplet generation process.

Table S1

Sequence of operations to perform droplet generation

		V1	V3	V4	V5	V7	V8	V9	V10	V11	V12	V13	V14	V15	V17
Step i	Release pressure	X	X	O	O	O	X	O	X	O	X	O	X	X	O
Step ii	Measure reagents	X	X	X	X	O	O	X	O	X	O	X	O	X	O
Step iii	Merge reagents	O	O	X	O	O	X	O	X	O	X	O	X	X	O
Step iv	Deliver droplet	O	O	X	O	O	X	O	X	O	X	O	X	O	O
Sealing step*	Sealing inlets/outlets	X	X	X	X	O	X	X	X	X	X	X	X	X	O

O: valve open; X: valve closed

* All valve numbering follows **Figure S1**. The valves not shown here are always closed during this process. The sealing step is inserted after each step, closing all inlet and outlet valves to account for valve response times.

Table S2

Sequence of operations to perform droplet generation for washing

		V1	V2	V3	V4	V5	V7	V9	V11	V13	V15	V17
Step 1	Release pressure	X	X	O	O	O	O	O	O	O	X	O
Step 2	Measure DI water	X	O	O	X	O	O	O	O	O	X	O
Step 3	Deliver droplet	O	X	O	X	O	O	O	O	O	O	O
Sealing step	Sealing inlets/outlets	X	X	O	X	O	O	O	O	O	X	O

O: valve open; X: valve closed

* All valve numbering follows **Figure S1**. The valves not shown here are always closed during this process. The sealing step is inserted after each step.

Adjustment of pH Condition

One of the unique features of our DMDG chip is its capability of pausing and restarting droplet generation at any time during the operation process. By stopping the droplet generation process, switching pH of the reaction mixtures can be achieved using an external microfluidic distribution chip connected to vials with different pH control buffer solutions. The entire changing pH control buffers and the subsequent cleaning process is automated and accomplished in less than 1 minute. Afterward the entire process resumed again to produce droplets with new a composition.

The volume ratio for [^{18}F]SFB, A2 Db and standard pH control buffer (pH 4, 4.5, 5, 5.5, 6, 8, 8.72, 10, 11, 12, 13) are fixed (1:1:1). All the three sections (**I**, **II** and **III**) have the same fixed volume (*ca.* 40 nL, 5 chamber units) for filling reagent. To change the pH control buffer automatically, the operation of DMDG chip was synchronized with the distribution chip. As an example (**Fig. S6 and Table S3**), pH buffer No.7 is provided from the distribution chip by opening valve P7. In order to switch to pH buffer No.8, valve P7 on the distribution chip is closed and valve P2 is opened to admit compressed nitrogen. At the same time, valves V14, V15 and V16 in the DMDG chip are opened. All pH buffer No.7 contained in the two chips and the tubing between them is pushed out to the waste by nitrogen. After a few seconds, valve P1 is opened to admit PBS buffer to clean the channel. Next, valve P2 is opened to admit compressed nitrogen and expel PBS buffer from the fluid path. Then valve P8 is opened to flow pH buffer No.8 into the DMDG chip for a few seconds. Valve V8 is then closed and the droplet generator cleaning cycle is performed, such that the DMDG chip is ready to generate the next droplets using this pH control buffer. In summary, using the droplet generator in combination with the pH control buffer distribution chip, droplets containing mixtures of labeling reagents at different pH values can be quickly and easily produced, and pH conditions can be rapidly optimized. In a

typical experiment, 11 different pH control buffers are available from an external solution distribution chip (**Fig. S6**).

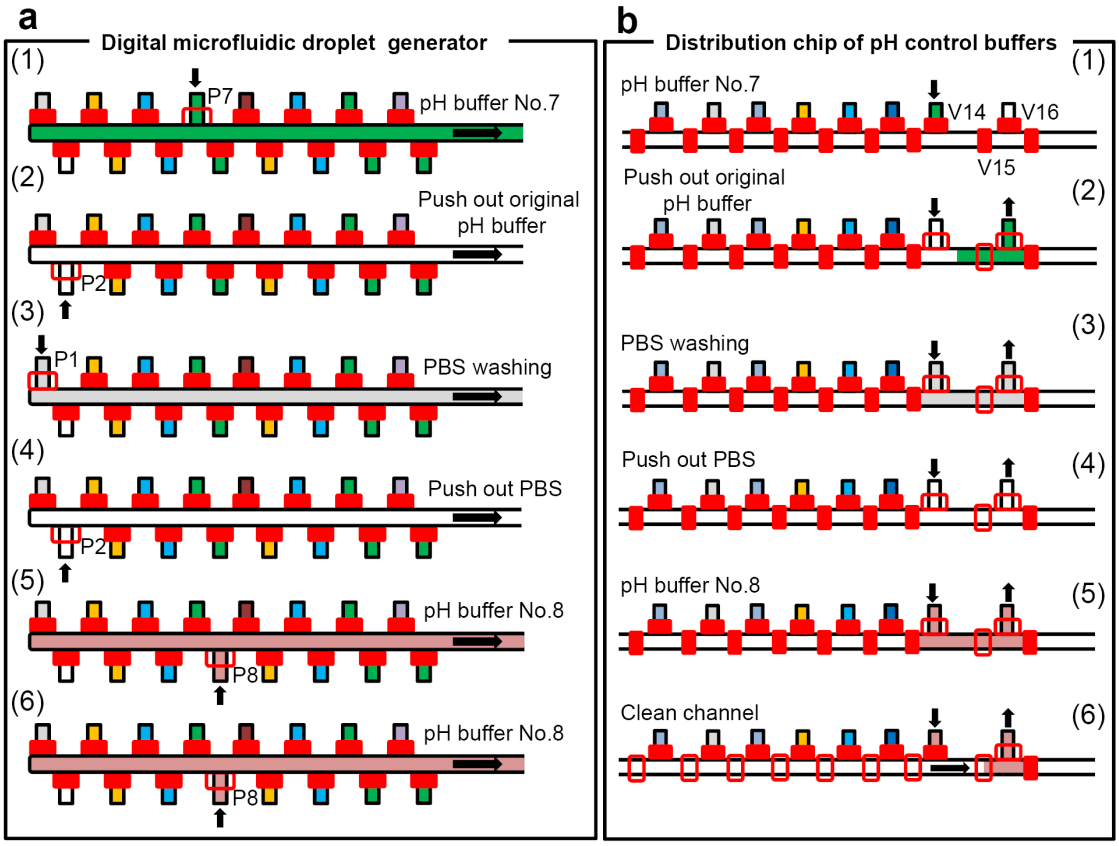

Figure S6. Schematic of the process of switching pH control buffer.

Table S3

Example sequence of operations to switch pH control buffer

		P1	P2	P7	P8	V1	V3	V5	V7	V9	V11	V13	V14	V15	V16
Step 1	pH buffer No.7	X	X	O	X	X	X	X	X	X	X	X	X	X	X
Step 2	Expel pH buffer	X	O	X	X	X	X	X	X	X	X	X	O	O	O
Step 3	Wash channel	O	X	X	X	X	X	X	X	X	X	X	O	O	O
Step 4	Expel wash buffer	X	O	X	X	X	X	X	X	X	X	X	O	O	O
Step 5	pH buffer No.8	X	X	X	O	X	X	X	X	X	X	X	O	O	O
Step 6	Clean chamber	X	X	X	O	O	O	O	O	O	O	O	X	O	O
Sealing step*	Sealing inlets/outlets	X	X	X	X	X	X	X	X	X	X	X	X	O	X

O: valve open; X: valve closed

* All valve numbering follows **Figures S1**. The valves not shown here are always closed during this process. The sealing step is inserted after each step.

pH Measurement

Due to the small volume of each droplet, the exact pH value of each droplet was subsequently estimated/determined by mixing the standard pH buffers, pH 7.4 PBS buffer and pH 8.7 borate buffer in the same volume ratios in larger quantities. The final pH of each solution was determined by a conventional pH meter (Accumet® AP62 pH/mV Meter, Fisher Scientific, USA). The final pHs of 11 different conditions were estimated to be 5.08, 6.60, 8.13, 8.42, 8.60, 8.68, 8.72, 8.88, 9.24, 9.42, and 10.00.

Optimization of pH on Chip

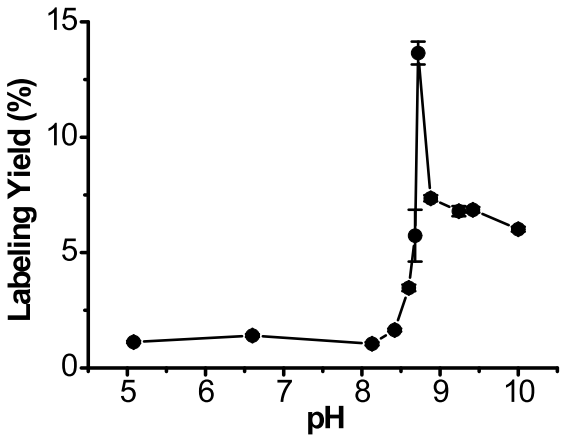

Figure S7. Screening optimal pH labeling condition (at 30°C, 5 min) using a DMDG chip. A2 Db (2 mg/mL) is stored in pH 7.4 buffer (n=3).

Adjustment of A2 Db Concentration

The flexible, microvalve-based DMDG chip is designed to facilitate adjustments of composition such that pH and biomolecule concentration can be independently controlled. From **Figure 1E**, the radioactive tag, biomolecule and pH control buffer are filled into section I, section II and section III respectively. All the three sections have the same fixed volume (*ca.* 40 nL, 5 chamber units). In order to change the concentration of biomolecule, section II is subdivided using microvalves into two chambers for biomolecule and dilution buffer (same buffer as that in which biomolecule is stored). For example, section II can contain two chamber units (*ca.* 16 nL) of biomolecule and the rest (three chamber units) with dilution buffer (**Fig. S8a**). Because the total droplet volume remains unchanged, only the concentration of biomolecule is affected by this dilution. If the pH of biomolecule solution is the same as the pH control buffer, the dilution factor of biomolecule can be extended from 1:5 to 1:10. This is achieved by merging section II and section III and using inlet 5 and inlet 6 sequentially to load biomolecule then dilution buffer (**Fig. S8b**). As an example, 8 chamber units can be filled with biomolecule at first. Then the biomolecule inlet is closed and the chamber is connected with the rest of 2 chamber units. pH control buffer would continue to fill the remainder of the 10 chamber units, resulting in a final biomolecule concentration that is 80% of the original stock solution. In the present study, the original biomolecule reagent stock was 2 mg/mL in pH 8.7 buffer, and final reaction concentrations from 0.13 mg/mL to 1.3 mg/mL could easily be produced on-chip.

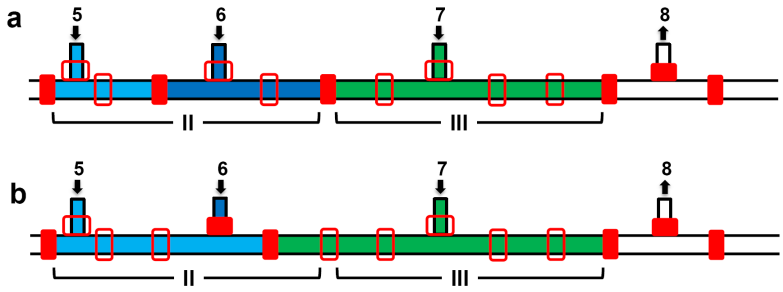

Figure S8. Adjusting concentration of A2 Db: (**a**) If pH buffer of A2 Db is different from pH control buffer (inlet 7), the concentration of A2 Db can only be adjusted by changing the ratio of A2 Db (inlet 5) and buffer 2 (inlet 6), which is the same buffer in which A2 Db is stored, in section II. (**b**) If A2 Db buffer is the same as pH control buffer, the concentration of A2 Db can be adjusted by changing the ratio of A2 Db (inlet) and pH control buffer (inlet 7) in section II and section III. (Inlet 6 is not used in this case.)

To determine the specific activity of [^{18}F]FB-A2 Db, its radioactivity was measured using a dose calibrator (CRC-25R, Capintec, Ramsey, NJ). The concentration (i.e. amount) of A2 Db is determined by UV absorption measurement (280 nm). Molecular weight of A2 Db and its extinction coefficient were calculated according to its amino acid sequence (ProtParam Tool, ExPASy, SIB, Swissland). Calculated specific activities (SAs) (Ci/mmol) were derived by dividing total radioactivity obtained after purification by mmoles of diabody in the labeling reaction (based on a molecular weight of 55,000 Da). It was also corrected by the radiochemical purity of final purified product determined by iTLC.

Scale-up Using Bench-scale Method

After optimizing pH and concentration, these labeling conditions can be scaled up. The same batch of PSCA A2 Db solution in borate/saline buffer (1 mg/mL, pH 8.7, 50 mM) and [^{18}F]SFB in pH 7.4 PBS buffer were used to conduct labeling reactions to compare the bench-scale method and microfluidic approach. Both of methods used the same conditions: one unit volume of [^{18}F]SFB and two unit volumes of anti-PSCA A2 diabody. After mixing and reacting for 5 min at 30^{o}C, the radiochemical yields were measured by iTLC and size exclusion HPLC (Biosep SEC S-2000; Phenomenex, Torrance, CA). For iTLC, the radiolabeled conjugates were evaluated by mobilization in normal saline. Strips were cut in half (bottom half: bound radiolabel, top half: free radiolabel) and counted in a gamma counter (Wizard 3; Perkin Elmer, Waltham, MA). Using this method, the radiochemical yields were 21.5% from the microfluidic chip and 22.1% from the vial. The radiochemical yields of the same batch of radiolabeled conjugates by size exclusion HPLC were 21.8% and 23.3%, respectively (**Fig. S9**). Radiolabeled diabody was separated from free [^{18}F]SFB and [^{18}F]FBA by a spin column (Micro Biospin 6 column (Bio-Rad, Hercules, CA), which had been pre-equilibrated with PBS and used according to the manufacture provided protocol). Following separation on the spin column, the radiochemical purity of [^{18}F]FB-A2 Db was greater than 95% (**Fig. S10**).

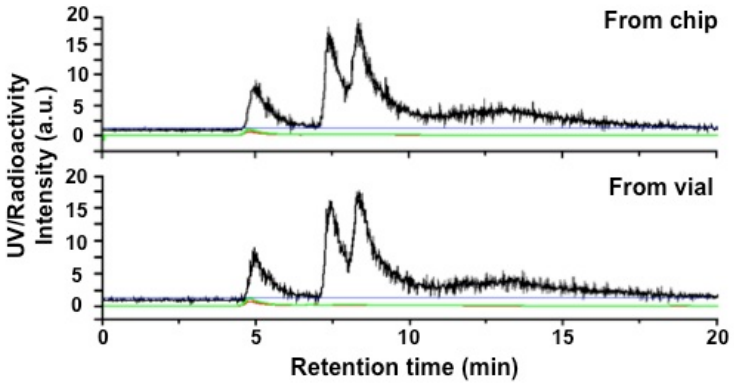

Figure S9. Size-exclusion chromatographic analyses of crude [^{18}F]FB-A2 Db obtained by the microfluidic chip approach and bench-scale method. The first peak is [^{18}F]FB-A2 Db . The labeling yields are 21.8% from the chip approach and 23.3 % from the bench-scale approach. [Radioactivity (black); UV trace: 254 nm (red) and 280 nm (green)].

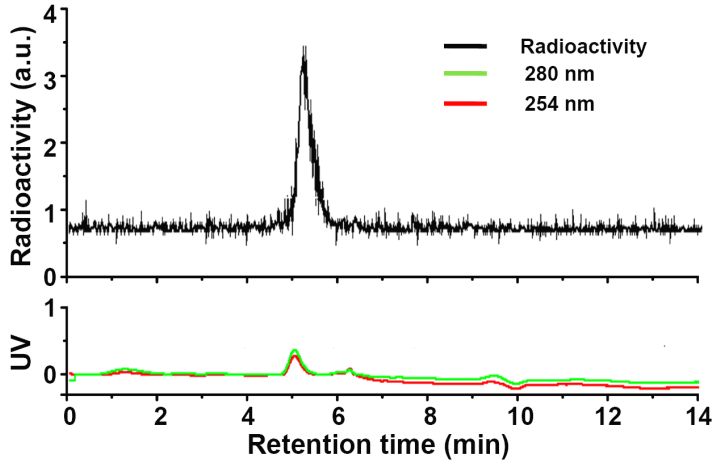

Figure S10. Size-exclusion chromatographic analyses of final purified [^{18}F]FB-A2 Db.

MicroPET/CT Imaging of Hydrolyzed [^{18}F]SFB

As a control experiment, 4-[^{18}F]fluorobenzoic acid ([^{18}F]FBA, i.e. hydrolyzed [^{18}F]SFB) was also injected into the tail vein of a tumor-bearing mouse and a microPET and CT scan were performed 2 hours post injection (**Figure S11**).

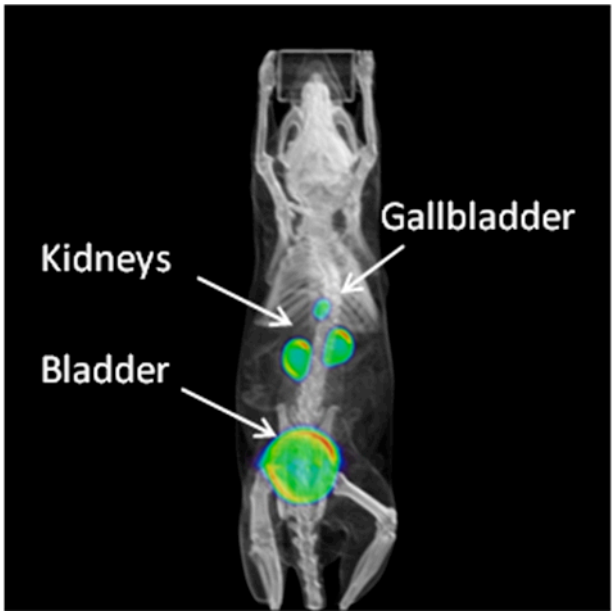

Figure S11. Co-registered microPET/CT scan images of a nude mouse injected with 4-[^{18}F]fluorobenzoic acid ([^{18}F]FBA, i.e. hydrolyzed [^{18}F]SFB) 2 h post tail vein injection.

Optimization of [^{18}F]SFB Labeling anti-HER2 Diabody

We also applied this microfluidic-based method to optimize the [^{18}F]SFB labeling of a different protein (an anti-HER2 diabody, the concentration of stock solution is ca 0.5 mg/mL). After screening for the optimal pH and concentration, it was fond that the optimal pH is around 8.6 and the optimal concentration is around 0.33 mg/mL (**Fig. S12**). Using this optimized labeling condition, we succeed obtaining the enough [^{18}F]FB-anti-HER2 Db (RLY=18.2%) for microPET studies in a xenografted mouse (MCF-7/HER2).

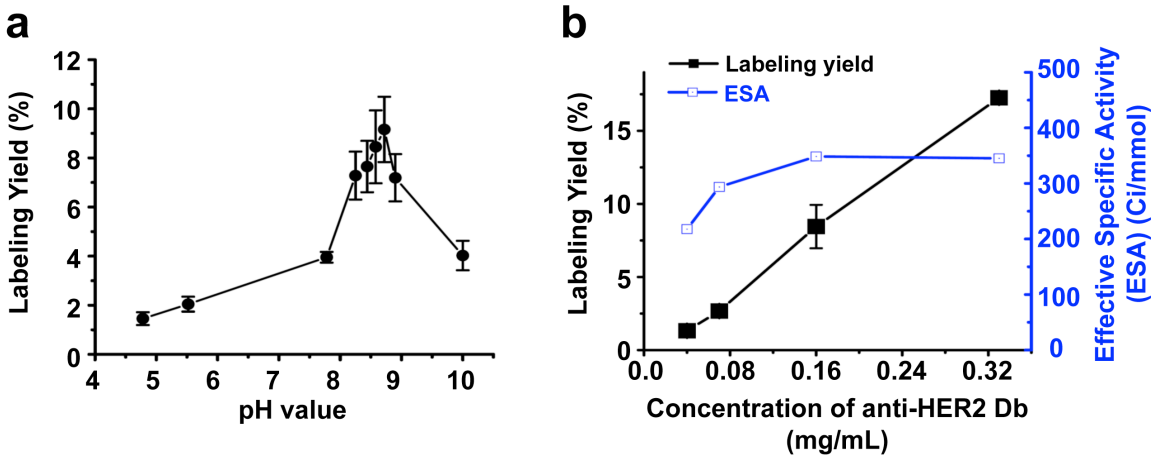

Figure S12. (a) Screen pH (n=3, anti-HER2 Db: 0.17mg/mL) and (b) concentration (n=3) of anti-HER2 Db using a microfluidic chip.

MicroPET/CT Imaging of [^{18}F]FB-anti-HER2 Diabody

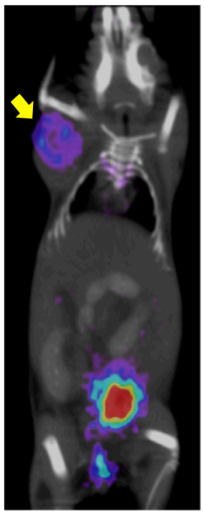

Figure S13. Co-registered microPET/CT scan images of a tumor-bearing mouse (MCF-7/HER2 over-expressing cells) injected with [^{18}F]FB-anti-HER2 Db (6 h p.i.).

Movie S1: Process of droplet generation-first droplet.

Movie S2: Change droplet composition on the fly.

Reference

1 Unger MA, Chou HP, Thorsen T, et al. Monolithic microfabricated valves and pumps by multilayer soft lithography. Science 2000; 288:113-16

2 Wang MW, Olam S, Liu K, et al. Microwave-assisted one-pot synthesis of N-succinimidyl-4-[^{18}F]fluorobenzoate ([^{18}F]SFB). Submitted.